

## Bio-ink properties and printability for extrusion printing living cells†

Cite this: *Biomater. Sci.*, 2013, **1**, 763

Johnson H. Y. Chung,<sup>a</sup> Sina Naficy,<sup>a</sup> Zhilian Yue,<sup>a</sup> Robert Kapsa,<sup>a,b</sup> Anita Quigley,<sup>a,b</sup> Simon E. Moulton<sup>\*a</sup> and Gordon G. Wallace<sup>\*a</sup>

Additive biofabrication (3D bioprinting) makes it possible to create scaffolds with precise geometries, control over pore interconnectivity and architectures that are not possible with conventional techniques. Inclusion of cells within the ink to form a “bio-ink” presents the potential to print 3D structures that can be implanted into damaged/diseased tissue to promote highly controlled cell-based regeneration and repair. The properties of an ‘ink’ are defined by its formulation and critically influence the delivery and integrity of structure formed. Importantly, the ink properties need to conform to biological requirements necessary for the cell system that they are intended to support and it is often challenging to find conditions for printing that facilitate this critical aspect of tissue bioengineering. In this study, alginate (Alg) was selected as the major component of the ‘bio-ink’ formulations for extrusion printing of cells. The rheological properties of alginate-gelatin (Alg-Gel) blends were compared with pre-crosslinked alginate and alginate solution to establish their printability whilst maintaining their ability to support optimal cell growth. Pre-crosslinked alginate on its own was liquid-like during printing. However, by controlling the temperature, Alg-Gel formulations had higher viscosity, storage modulus and consistency which facilitated higher print resolution/precision. Compression and indentation testing were used to examine the mechanical properties of alginate compared to Alg-Gel. Both types of gels yielded similar results with modulus increasing with alginate concentration. Decay in mechanical properties over time suggests that Alg-Gel slowly degrades in cell culture media with more than 60% decrease in initial modulus over 7 days. The viability of primary myoblasts delivered as a myoblast/Alg-Gel bio-ink was not affected by the printing process, indicating that the Alg-Gel matrix provides a potential means to print 3D constructs that may find application in myoregenerative applications.

Received 14th January 2013,  
Accepted 24th April 2013

DOI: 10.1039/c3bm00012e

[www.rsc.org/biomaterialsscience](http://www.rsc.org/biomaterialsscience)

### 1. Introduction

An emerging approach to create complex three dimensional constructs containing biological cells is by a process referred to as ‘biofabrication’ or ‘bioprinting’, using an appropriately formulated bio-ink. Several biofabrication methods have been used to create 3D scaffolds for tissue engineering applications.<sup>1,2</sup> 3D bioplotting, first introduced by Landers *et al.*<sup>3,4</sup> is an extrusion based method that can continuously dispense materials (*i.e.*, ‘ink’) and biological cells from a movable dispensing head or onto a moving stage to form patterns

predesigned through computer-aided design (CAD) tools.<sup>4</sup> This method has less geometrical limits than most of the conventional methods and can deposit material and cells within tens of minutes.<sup>5</sup>

Ink development can be considered as one of the most challenging aspects in the bioprinting process. An ‘ideal’ ink should satisfy biological needs from the cell compatibility point of view, but also the physical and mechanical needs of the printing process itself. Physically, the ink should exhibit gel-like characteristics or be sufficiently viscous to be dispensed as a free standing filament. However, if the gel is too strong, large shear forces required to eject the ink can result in cell death and gel fracture.<sup>6</sup> Mechanically, the individual printed filaments require sufficient strength and stiffness to maintain structural integrity after printing. Lastly, the formulation should not be cytotoxic, allowing cell adhesion and proliferation. In some cases, degradation of the scaffold in a controlled manner over time will be appropriate. Hydrogels are polymeric materials commonly used in tissue engineering due to their low cytotoxicity and structural similarity to the

<sup>a</sup>ARC Centre of Excellence for Electromaterials Science, Intelligent Polymer Research Institute, University of Wollongong, Wollongong, NSW 2522, Australia.

E-mail: [gordon\\_wallace@uow.edu.au](mailto:gordon_wallace@uow.edu.au), [smoulton@uow.edu.au](mailto:smoulton@uow.edu.au);

Fax: +61 2 4221 3114; Tel: +61 2 4221 3127, +61 2 4298 1443

<sup>b</sup>Centre for Clinical Neuroscience and Neurology Research and Department of Medicine, The University of Melbourne, St. Vincent's Hospital, Fitzroy, Victoria 3065, Australia

†Electronic supplementary information (ESI) available. See DOI: 10.1039/c3bm00012e

extracellular matrix (ECM).<sup>7</sup> The highly hydrated network structure permits the exchange of gases and nutrients and makes them an attractive option for the formation of “inks” for bioprinting. Blending of hydrogels provides an opportunity by which properties specific to each respective hydrogel component can be combined to tailor the overall hydrogel towards facilitating specific requirements.<sup>8,9</sup>

Alginates (Alg) are naturally occurring polysaccharides isolated from brown algae with linear blocks of (1,4)-linked  $\beta$ -D-mannuronate (M) acid and  $\alpha$ -L-guluronic acid (G) residues.<sup>10,11</sup> Gel formation can be achieved through binding of divalent cations with guluronic residues of the alginate chain, subsequently forming junctions with adjacent chains creating an egg-box structure.<sup>10,12</sup> The viscosity of alginate solution depends on the average molecular weight ( $M_w$ ), molecular weight distribution, average chain segment ratio (G to M ratio), concentration of the polymer and the pH of the solution.<sup>11,12</sup> Due to the structural similarity of alginate to ECM, these gels are used in cell delivery vehicles,<sup>13</sup> matrices for tissue engineering,<sup>14</sup> drug delivery beads and ECM models for cell experiments.<sup>15</sup> Gelatin, a denatured type of collagen, has been widely used in wound dressing, as pro-angiogenic matrices and absorbent pads for surgical applications.<sup>16–18</sup> At physiological temperature (37 °C), gelatin is a solution, but can reversibly form a gel when cooled (<29 °C). This is due to a conformational change from coil to helix that leads to chain association and eventually the formation of a three-dimensional network.<sup>2,19–21</sup> The viscosity of an alginate solution and thereby printability, can also be controlled by incorporating gelatin and modulating the mixing temperature during printing to form a gel that retains biological aspects of the original alginate solution while satisfying physical extrusion criteria.

Alginate-gelatin (Alg-Gel) blends have been reported as potential drug delivery carriers,<sup>8,9</sup> enzyme immobilisation beads,<sup>22</sup> wound dressing fibres,<sup>23</sup> and sponges for tissue matrices.<sup>24</sup> Among the studies related to bioprinting, Yan and co-workers<sup>25–27</sup> have attempted to print 3D scaffolds from alginate-gelatin blends. Here, we elaborate this approach with particular attention paid to the ink properties required for effective printing with respect to both the delivery and integrity of structure formed. Interestingly, there have been limited studies aimed at understanding the specific ink properties suitable for extrusion printing. This study establishes a systematic approach to characterise the specific requirements needed to print a 3D scaffold successfully for tissue engineering (TE). The printability of ink formulations was assessed by comparing a viscous solution, semi-crosslinked gel and hybrid hydrogels. Alginate was selected as the major component of the ink formulations used in this work due to its potential in biomedical applications, and its versatility in generating a range of possible inks by ionically crosslinking it or blending with another component. The techniques examined here provide the criteria and tools by which the printability of a hydrogel-based ink can be evaluated. In addition, the mechanical properties and cell compatibility of the optimum ink formation will be investigated.

## 2. Materials and methods

### 2.1 Materials

Alginate sodium salt ( $M_w \sim 50\,000$  Da, M/G ratio of 1.67, viscosity of 100–300 cP for 2 w/w solution, 25 °C) and gelatin ( $M_w \sim 50\,000$ – $100\,000$  Da, type A from bovine skin) were obtained from Sigma-Aldrich Pty Ltd. Other reagents were all analytical grade and used as received.

### 2.2 ‘Ink’ preparation

To prepare the ink solution, three different concentrations of sodium alginate solution (1, 2 and 4% w/v) were prepared in phosphate buffered saline (PBS, pH 7.4) and blended with 10% w/v gelatin solution (4 parts alginate solution: 1 part gelatin solution, kept constant for all blended samples). The ink solution was mixed using vortex and centrifuged for 1 min (1000 rpm) to remove air bubbles. The ink solution was then transferred into syringe barrels or appropriate moulds for characterisation and cooled on ice for 15 min. Ink solutions comprising alginate at 1, 2 or 4% blended with gelatin were labelled as 1% Alg-Gel, 2% Alg-Gel and 4% Alg-Gel respectively, while alginate solutions without added gelatin were labelled as 1% Alg, 2% Alg and 4% Alg respectively. For comparison, an alginate solution (4% w/v) pre-mixed with calcium chloride (0.2% v/v) was also prepared and labelled 4% Alg + Ca<sup>2+</sup>.

### 2.3 Fabrication of scaffolds

Samples were extrusion printed using a custom modified computer numerical control (CNC) milling machine (Sherline Products, CA). The system was equipped with a three-axis positioning platform and designed using EMC2 software (LinuxCNC). An attachment for syringe deposition was built and connected to a controllable gas flow regulator (1–100 psi). The regulator was controlled using a Pololu SciLabs USB-to-serial microcontroller and with an in-house software interface. The ink solution was loaded into a disposable syringe (Nordson EFD), kept at 5 °C and fitted with a 200  $\mu$ m diameter nozzle. Three layers of the ink solution were extruded onto a glass slide at a feed rate of 100 mm min<sup>-1</sup>, with strands spacing of 1 mm, to a final size of 10 mm  $\times$  10 mm. The gas pressures used for extruding the various ink solutions were selected to produce the most reproducible and defined structure and were 4, 8 and 9.5 psi for 1%, 2% and 4% Alg-Gel respectively. 4% Alg + Ca<sup>2+</sup> was printed at RT (25 °C, 2 psi). Samples required for further characterisation were ionically crosslinked in 2% w/v CaCl<sub>2</sub> for 10 min. The macroscopic structure of extruded scaffolds was imaged using Leica M205A optical microscope (Leica Microsystems, Germany).

### 2.4 Ink consistency measurement

The consistency of the ink solutions were measured using the method described by Cohen *et al.*<sup>28</sup> The method was based on measuring the variations in extrusion force during deposition of ink in real time. Ink solutions were loaded into a syringe with the plunger connected to the upper clamp of an EZ-S

mechanical tester (Shimadzu, Japan). The measurements were performed in compression mode while the nozzle end of the syringe (200  $\mu\text{m}$  in diameter) was held perpendicularly in position by a plastic rack. A 10 N load cell was used and the testing was carried out by applying a constant strain at 0.2  $\text{mm s}^{-1}$  and recording the force over time (see ESI†). Distilled water was used as a control for the experiment and regions where the force showed consistent fluctuations over 300 s was used.

## 2.5 Rheology

The rheological behaviour of ink solutions was analysed using an AR-G2 rheometer (TA Instruments, DE) equipped with a Peltier plate thermal controller. A 2°/40 mm cone and plate geometry was used in all measurements (see ESI†). The solutions were allowed to reach the equilibrium temperature for 1 min prior to performing the experiments. Storage modulus ( $G'$ ) and loss modulus ( $G''$ ) were measured as a function of temperature and frequency by varying, respectively, temperature (at a constant frequency) and frequency (at a constant temperature). Temperature sweep experiments were conducted at a rate of 6  $^{\circ}\text{C min}^{-1}$  from 50  $^{\circ}\text{C}$  to 5  $^{\circ}\text{C}$ , at a fixed strain and frequency of 1% and 1 Hz respectively. Frequency sweep experiments (5  $^{\circ}\text{C}$  for Alg-Gel, 25  $^{\circ}\text{C}$  for all Alg) were conducted at a fixed strain of 1% from 0.01 to 10 Hz. A temperature of 5  $^{\circ}\text{C}$  was selected for conducting experiments on Alg-Gel to ensure the ink maintains a gel-like structure.

## 2.6 Mechanical properties

The modulus of alginate and alginate-gelatin samples was determined using both compression and indentation tests. Ink solutions were casted in custom-made moulds (compression: cylindrical, 10 mm ID, 4 mm in thickness; indentation: square, 10 mm  $\times$  10 mm  $\times$  2 mm). The samples were crosslinked in 2% w/v  $\text{CaCl}_2$  for 10 min, washed and equilibrated in Dulbecco's modified eagle medium (DMEM, Sigma Aldrich) supplemented with 10% foetal bovine serum and 1% penicillin/streptomycin (P/S) for 30 min to remove the excess calcium ions. For compression testing, the diameter and thickness of each sample was measured using a digital micrometer. Each sample was tested at a strain rate of 2  $\text{mm min}^{-1}$  using the EZ-S mechanical tester fitted with a 10 N load cell (see ESI†). The initial linear slope of stress-strain curve was used to calculate the compression modulus ( $E_{\text{comp}}$ ). At least three different samples were used for each composition and the average values are reported.

A flat stainless steel indenter (1 mm in diameter) was used along with a 2 N load cell to perform the indentation test at a rate of 0.1  $\text{mm min}^{-1}$ . At least three different samples were used for indentation testing and the test was carried out on a minimum of 4 different points for each sample. The indentation modulus ( $E_{\text{ind}}$ ) was calculated from the recorded force and the indenter displacement. The applied force ( $F$ ) can be related to the indentation depth ( $d$ ) by taking in account the reduced modulus ( $E^*$ ) and the indenter geometry (radius  $a$ ):

$$F = 2aE^*d \quad (1)$$

where the reduced modulus in eqn (1) can be expressed as a function of the indenter modulus ( $E_1$ ) and the substrate modulus ( $E_2$ ):<sup>29</sup>

$$(E^*)^{-1} = (1 - \nu_1^2)E_1^{-1} + (1 - \nu_2^2)E_2^{-1} \quad (2)$$

here,  $\nu_1$  and  $\nu_2$  are the Poisson's ratios of the indenter and the substrate, respectively.  $(1 - \nu_1^2)E_1^{-1}$  of eqn (2) becomes negligible when indenter is much stiffer than the substrate. For swollen hydrogels  $\nu_2$  is taken as 0.5, and eqn (1) and (2) become:

$$F \sim (8/3)aE_2d \quad (3)$$

Comparisons between Alg and Alg-Gel were made using a two-way analysis of variance (ANOVA). A  $p$ -value  $< 0.05$  was used to indicate a significant difference.

## 2.7 Degradation analysis

Degradation study was undertaken by monitoring the loss in material strength of the samples in cell culture medium at 37  $^{\circ}\text{C}$  (Dulbecco's Modified Eagle Medium supplement foetal bovine serum (10%) and penicillin/streptomycin (1%)) using compression and indentation tests. Materials for degradation studies were cast and the experiment conducted as previously described in Section 2.6. Measurements were taken after 1, 4, 7 and 14 days incubated in cell culture media with fresh media being replenished at every second day. At every time point for measurement, samples were tested by indentation first followed by compression testing.

## 2.8 Cell compatibility

In order to facilitate efficient cell attachment and proliferation within the alginate-based scaffolds, the peptide sequence GRGDS (Auspep) was covalently linked to the alginate using aqueous carbodiimide chemistry under sterile conditions.<sup>30–32</sup> Briefly, sodium alginate was dissolved in MES buffer (0.1 M, 0.3 M NaCl, pH = 6.5). 1-Ethyl-3-(3-dimethylaminopropyl) carbodiimide (EDC, Sigma-Aldrich) and  $N$ -hydroxysulfosuccinimide (sulfo-NHS, Sigma-Aldrich) were added to activate 5% of the carboxylic acid groups of alginate. The solution was stirred for 15 min followed by addition of peptide where the reaction was allowed to proceed for 24 h. The product was then dialysed for 4 days, lyophilised and stored at  $-80^{\circ}\text{C}$ . The grafting procedure was conducted accordingly to the study by Rowley *et al.*,<sup>30</sup> where they have optimised the chemistry with reaction efficiency reaching up to 80%. Based on values reported by Rowley *et al.*<sup>30</sup> and the alginate molecular weight (given by the manufacturer), the average number of peptide grafted per alginate chain was calculated to be 8 grafts per chains.

Primary cells used to conduct biological assays in this study were derived from two week old C57BL10/J back-crossed C57BL6-(GTRosa) mice. After euthanasia by cervical dislocation, the muscles were removed from the mice and macerated with sharp scissors in Hams F10 media devoid of serum. Primary myoblasts were then cultured in Hams F10 media supplemented with foetal bovine serum (20%), bFGF (2.5  $\text{ng ml}^{-1}$ ),

L-glutamine (2 mM) and penicillin/streptomycin (1%, P/S) as described elsewhere.<sup>33</sup> A 2% Alg-Gel ink solution was prepared as described previously (Section 2.2) under sterile conditions. Briefly, alginate-GRGDS was mixed with appropriate amounts of gelatin and BL6 primary myoblast at a cell density of  $5 \times 10^5$  cells  $\text{ml}^{-1}$ . The ink solutions were printed onto glass slides at 3 different pressures denoted as P1 (8 psi), P2 (16 psi) and P3 (24 psi) and crosslinked in 2% w/v  $\text{CaCl}_2$  for 10 min. To determine the viability of printed cells, samples were stained with calcein AM and propidium iodide (PI). In brief, samples were incubated with calcein AM for 10 min in dark, washed with cell culture media and stained with PI for 2 min. Samples were imaged using a Leica DM IL fluorescent microscope (Leica Microsystems, Germany) and analysed using Image J software. The viability of printed samples was tested 1 h and 48 h after printing. Results are presented as mean  $\pm$  standard deviation. Differences between groups were analysed using Tukey's method. A  $p$ -value  $< 0.05$  was used to indicate a significant difference.

### 3. Results

#### 3.1 Printability

The printability of the ink solutions was assessed using various techniques such as rheology, ink consistency measurements and a comparison between the sample dimensions inputted into the software and sample dimensions after fabrication. First, flow properties of the ink solutions were examined by rheology. Frequency sweep measurements of Alg and Alg with added calcium (4% Alg +  $\text{Ca}^{2+}$ ) during ink preparation were compared and shown in Fig. 1A. Clearly, alginate premixed with calcium exhibited gel-like behaviour, as indicated by the higher storage modulus ( $G' > G''$ ) across the frequencies tested. On the other hand, a 4% Alg solution behaves simply as a viscous fluid, where  $G''$  is dominant across all frequencies. The dominance of loss modulus ( $G''$ ) means that the ink made purely of Alg behaves as a fluid with insufficient storage

**Table 1** Dimensions of as-printed structures

	4% Alg + $\text{Ca}^{2+}$	Alg-Gel		
		1%	2%	4%
Pore-diameter (mm)	$0.24 \pm 0.37$	$0.30 \pm 0.25$	$0.61 \pm 0.24$	$0.61 \pm 0.11$
Filament width (mm)	$0.64 \pm 0.14$	$0.60 \pm 0.19$	$0.32 \pm 0.18$	$0.37 \pm 0.32$
Filament spacing (mm)	$1.1 \pm 0.09$	$1.09 \pm 0.26$	$1.04 \pm 0.12$	$1.01 \pm 0.09$

Intended dimension parameters: pore diameter = 1 mm; needle width = 0.2 mm; filament spacing = 1 mm.

modulus ( $G'$ ) to hold the shape of printed ink. As a result, attempts to use 4% Alg ink solutions to produce a 3D scaffold were not successful. Scaffolds printed using 4% Alg +  $\text{Ca}^{2+}$  is shown in Fig. 1B and detailed in Table 1. The smaller pore diameter and wider filament width compared to the intended extruding conditions suggested that this ink solution was not suitable for printing as the ink was still lacking the required storage modulus to hold the structure together and reduce the flow of the material.

As 4% Alg +  $\text{Ca}^{2+}$  was not a suitable candidate for printing defined structure, Alg-Gel ink solutions were examined as an alternative formulation for printing. The rheological behaviours of Alg-Gel inks are shown in Fig. 2. Prior to gelation ( $T > 25$  °C), both pure gelatin and 2% Alg-Gel solutions showed a typical fluid-like behaviour ( $G'' > G'$ ), as shown in Fig. 2A. Upon cooling,  $G'$  for both solutions increases rapidly and eventually crosses over  $G''$  showing characteristics of a gel-like structure. The gelation temperature (where  $G'$  and  $G''$  cross over) for gelatin occurs around room temperature ( $\sim 25$  °C), while Alg-Gel solutions exhibited a lower gelation temperature of around 11 °C. This suggested that printing of Alg-Gel ink solutions should be conducted at low temperatures to ensure the solutions exhibit gel-like behaviours. Similar to the frequency sweep measurements of 4% Alg +  $\text{Ca}^{2+}$  (Fig. 1A), ink solutions of 2% Alg-Gel (Fig. 2B) also showed a dominant  $G'$  over  $G''$  across all frequencies. However, the storage

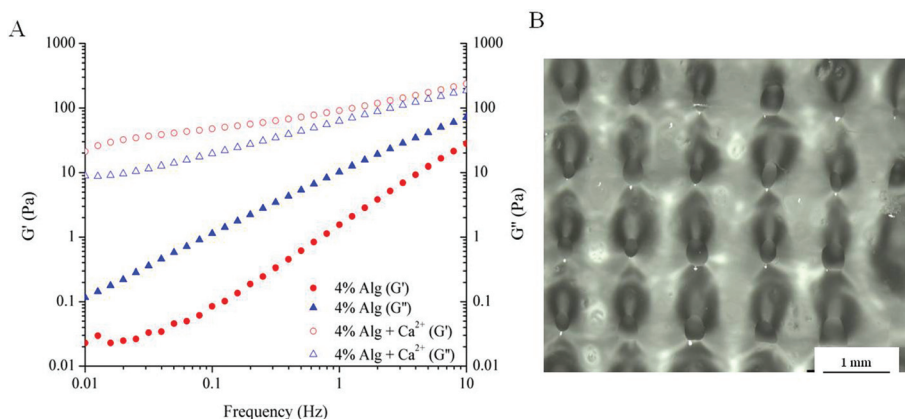


**Fig. 1** Printability of alginate. (A) Frequency sweep measurements of alginate and alginate with calcium added during ink preparation; (B) as-printed scaffold using 4% Alg +  $\text{Ca}^{2+}$  ink solution.

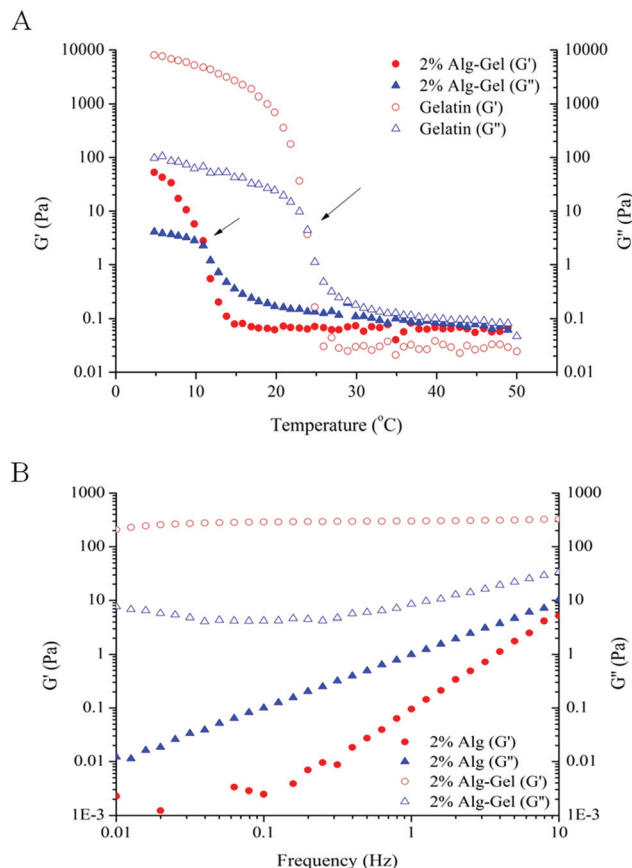


**Fig. 2** Rheological measurements. (A) Temperature sweep measurements comparing Alg-Gel with gelatin. Gelation temperature indicated by the temperature where  $G'$  intersects  $G''$  (indicated by arrows); (B) frequency sweep measurements comparing 2% Alg to 2% Alg-Gel.

modulus of 2% Alg-Gel (Fig. 2B) was an order of magnitude higher than that of 4% Alg +  $\text{Ca}^{2+}$  (Fig. 1A), which could indicate a viscoelastic behaviour more suitable for extrusion printing. Of note, unlike the 4% Alg +  $\text{Ca}^{2+}$  the storage modulus of 2% Alg-Gel remains almost independent of frequency, indicating the presence of a profound elastic element in the ink viscoelastic behaviour.

Using Alg-Gel ink solutions, the printing of scaffolds from three different alginate concentrations (1, 2, and 4% w/v) were compared and are shown in Fig. 3. A summary of the dimensions of the printed scaffolds are presented in Table 1. Compared to 4% Alg +  $\text{Ca}^{2+}$ , Alg-Gel ink solutions showed better resolution with respect to pore diameter and filament width. Increasing alginate concentrations increases the pore diameter and decreases the filament width due to the increase in viscosity and storage modulus of the ink. Both as-printed scaffolds using 2% Alg-Gel (Fig. 3B) and 4% Alg-Gel (Fig. 3C) demonstrated well defined structures that were more similar to the intended dimensions (Table 1). After crosslinking, printed scaffolds were mechanically robust enough to handle (Fig. 3E).

The consistency of ink solutions was compared and is shown in Fig. 4. The initial sharp increase in force due to plunger-syringe wall friction was omitted from the results and

regions where the force variations become constant were used. Being a purely Newtonian fluid with low viscosity, water showed a constant extrusion force around 2.5 N over time. Contrary to this, 4% Alg +  $\text{Ca}^{2+}$  showed greater fluctuations in extrusion force indicating greater heterogeneity within the solution. The inconsistent nature of 4% Alg +  $\text{Ca}^{2+}$  ink flow could also be a contributing factor to the poor printability and greater variations in pore diameter of scaffolds made from this ink. Interestingly, 4% Alg-Gel ink solution displayed minimal fluctuations in extrusion force. While greater in magnitude, the extrusion force displayed a uniform fluctuation profile more similar to that of water than alginate. This result suggests that the blending of gelatin with alginate may have assisted the ink to gel more uniformly when cooled, yielding overall gel properties more favourable for higher print resolution than alginate without gelatin.

### 3.2 Mechanical properties

In order to examine the properties of structures fabricated from these ink solutions, samples were cast and crosslinked. The modulus of Alg and Alg-Gel samples with varying Alg content is shown in Fig. 5A and 5B respectively. Increasing Alg concentration significantly increases both the indentation and compression modulus of Alg and Alg-Gel. The indentation modulus of 4% Alg-Gel was lower than 4% Alg ( $p = 0.0344$ ), however no significant differences were observed between Alg and Alg-Gel at concentrations of 1% ( $p = 0.9911$ ) and 2% ( $p = 0.6670$ ). Similar trends were observed using compression testing and there was no significant differences ( $p > 0.05$ ) between Alg and Alg-Gel samples.

The degradation behaviour in cell culture medium over 2 weeks *in vitro* was investigated through changes in material stiffness. The percentage of modulus remaining as a function of time and the values of indentation and compression modulus at each time point are presented in Fig. 6 and 7 respectively. Indentation testing could only be performed on the first few days for 1% Alg and 1% Alg-Gel as these samples became very weak over the time and did not have a flat surface for accurate measurements. In general, a trend of decreasing modulus with time can be seen for 2 and 4% samples. Alg-Gel samples also showed a lower modulus compared to their relative controls at each time point measured which can be due to the dissociation of gelatin network at 37 °C (mass loss of 1% Alg and 1% Alg-Gel was 14% and 61% respectively after 10 days). Using indentation, a localised part at the sample surface (~1 mm) was tested and a slower decrease in modulus can be seen from 4% Alg samples compared to 2% Alg (Fig. 6A). A similar behaviour can be observed in Alg-Gel samples (Fig. 6B). There were no noticeable differences between rates at which modulus decreased when comparing Alg to Alg-Gel samples with all samples showing close to 50% drop in modulus after 4 days in cell culture medium (Fig. 6C). The overall modulus of the samples was tested using compression (Fig. 7). Clearly, it can be seen that the modulus for all samples at each time point, especially day 14, were much less than the modulus measure by indentation. This could be due

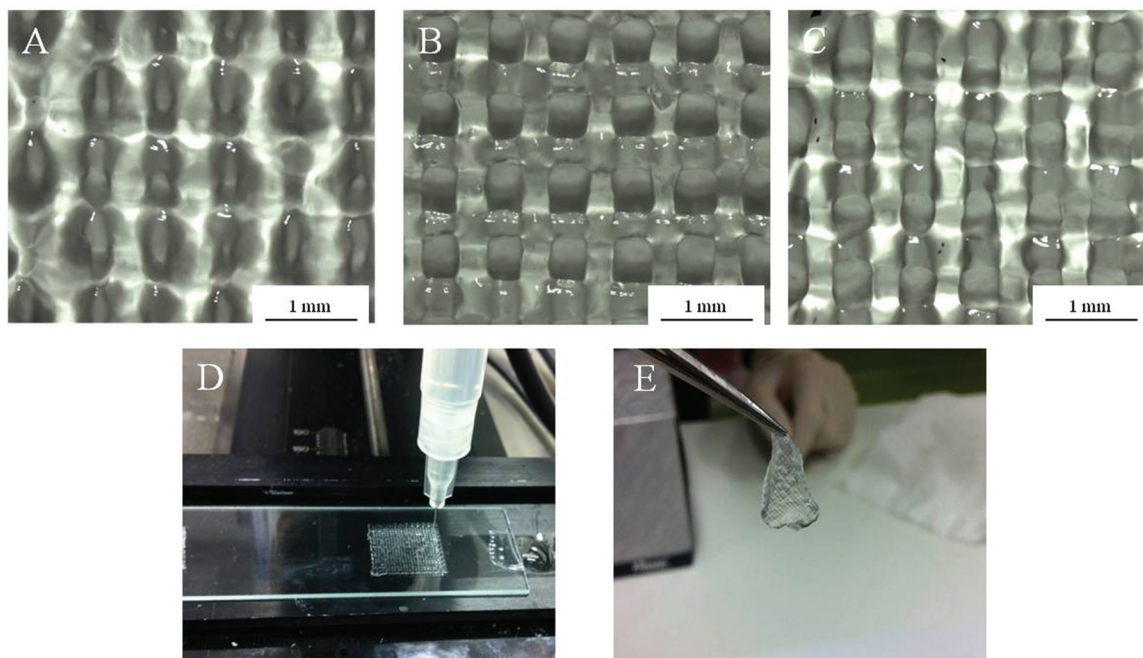


**Fig. 3** Structure of as-printed scaffolds using (A) 1% Alg-Gel; (B) 2% Alg-Gel; (C) 4% Alg-Gel ink solutions; (D) extrusion printing of Alg-Gel; (E) 2% Alg-gel after crosslinking in calcium chloride.

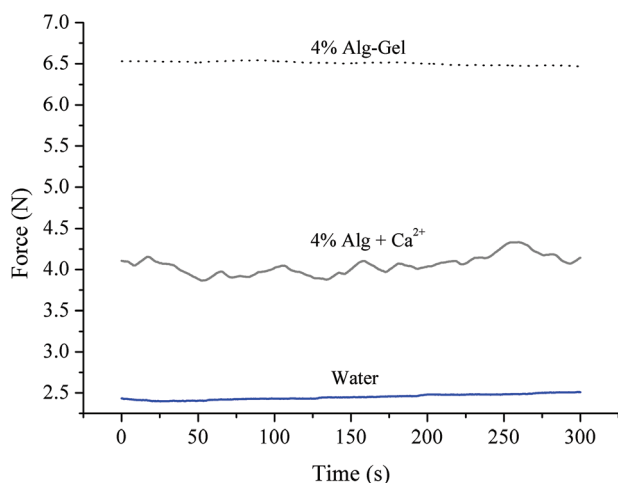


**Fig. 4** Consistency measurements of Alg-Gel and Alg + Ca<sup>2+</sup> ink solutions. Water was used as control.

to the difference in techniques where compression considers the entire sample, while indentation only measures a localised portion of the sample up to a certain depth. Similar to indentation, Alg and Alg-Gel samples decrease in stiffness over time regardless of alginate concentration.

### 3.3 Cell viability

A preliminary evaluation of the viability of myoblasts within Alg-Gel was conducted through a live/dead assay and shown in Fig. 8A. One hour following extrusion, no significant differences in cell viability (95% for P1, 97% for P2 and 92% for P3)

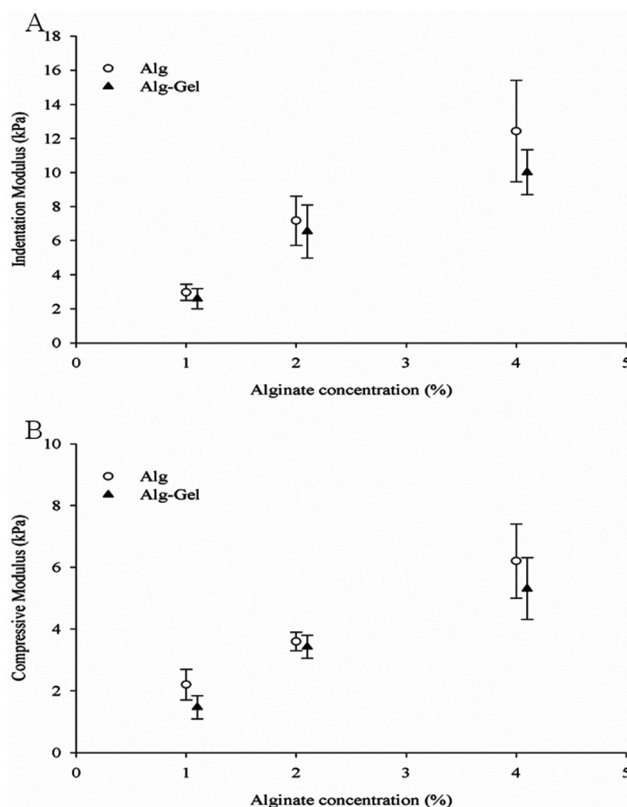


**Fig. 5** Modulus measurements of Alg and Alg-Gel using (A) indentation; and (B) compression. Data represents mean  $\pm$  s.d.

occurred between cells subjected to the 3 pressures applied respectively. In addition, the cell viability evident immediately

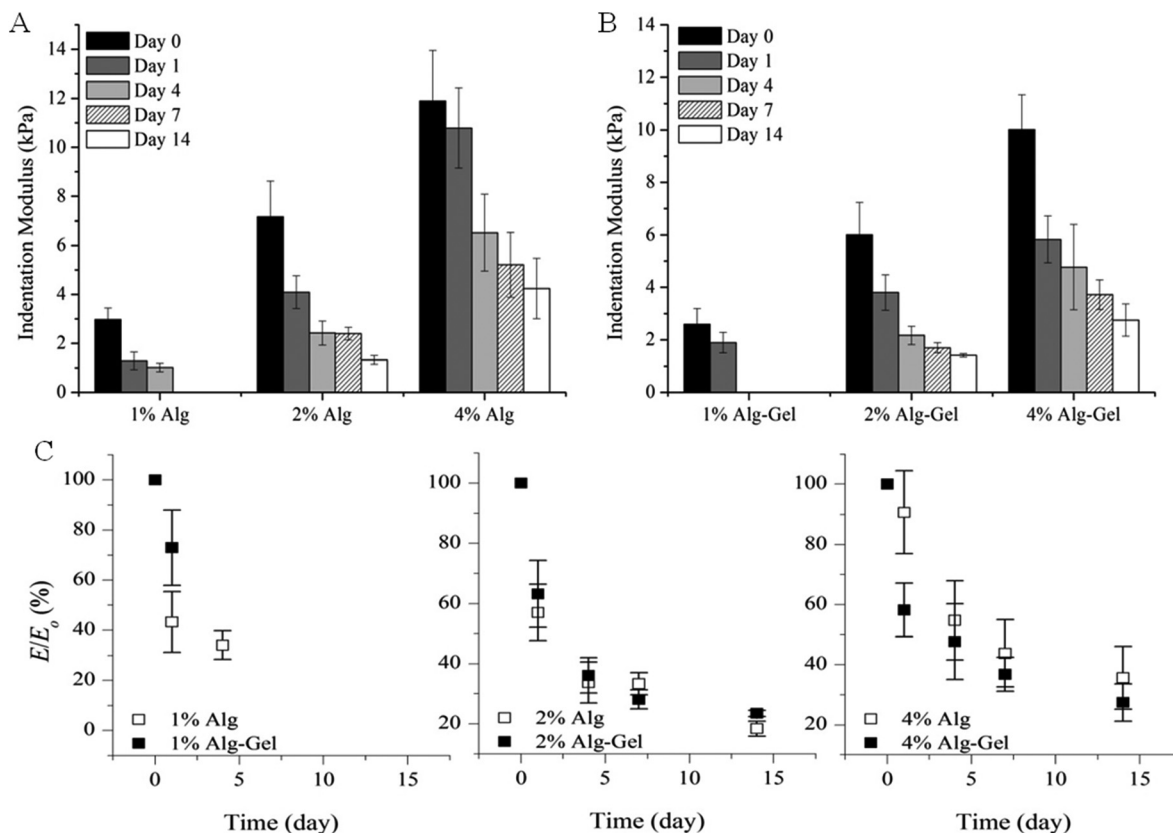


**Fig. 6** Indentation modulus of (A) Alg; and (B) Alg-Gel in cell culture medium over 14 days. (C) Modulus remaining. Expressed as a percentage of the modulus ( $E/E_0$ ) at the specified time point relative to the initial modulus at day 0. Data represents mean  $\pm$  s.d.

following extrusion was maintained for a further 48 hours (95% for P1, 98% for P2 and 96% for P3).

## 4. Discussion

Conventional techniques for scaffold fabrication often yield uncontrolled and imprecise scaffold geometries, especially in relation to pore sizes, pore size distribution, and pore interconnectivity. Using 3D biofabrication techniques such as bioplotting, structures or scaffolds with highly accurate 3D geometries can be fabricated in a controlled environment. Further to this, the ability to deposit cell-laden hydrogels potentially facilitates homogeneous distribution or positioning of cells, with the concomitant capability to seed cells or multiple cell types at discrete regions within the structure.<sup>34,35</sup> Alginate was selected as the major component of the ink formulation used in this study for its ease of gelation, cell compatibility and good stability as a three-dimensional structure.<sup>28</sup> Most importantly, alginate has the capacity to undertake chemical modifications that improves printability and the bioactivity, such as functionalising with RDG peptide,<sup>11</sup> along with well-known biocompatibility.

To satisfy the rheological requirements for extrusion printing, the viscosity of alginate can be varied through modulation of the alginate concentration or by pre-crosslinking the ink

before printing. Ionic crosslinking of alginate can be achieved through the addition of divalent cations such as  $\text{Ca}^{2+}$ . It is well documented that these divalent cations bind to the guluronic residues of alginate chains which can then form junctions with adjacent chains creating an egg-box structure.<sup>11,36</sup> It can be seen from rheological measurements (Fig. 1) that the presence of calcium ions during preparation can create an ink solution that is partially gelled with higher storage modulus than alginate in solution alone. However, the low resolution and fluid-like properties of the printed scaffolds using this formulation (Fig. 1B) suggested that the pre-crosslinked alginate ink was not suitable for printing. In addition, the calcium ions required for ink preparation are osmolytic and otherwise toxic to cells beyond certain concentrations. Calcium ions are important in a variety of cellular processes such as enzyme activity, muscle contraction and cell proliferation.<sup>37</sup> However, a low calcium concentration (2 mM) must be maintained in the cytoplasm which can otherwise disrupt homeostasis, leading to cell death.<sup>36,38</sup> Although calcium is first mixed with alginate prior to the addition of biological cells during ink preparation, excess  $\text{Ca}^{2+}$  can still have a negative impact on cell viability.

Ink homogeneity was also considered an important prerequisite to obtain ink printability. As  $\text{CaCl}_2$  is highly soluble in aqueous solutions it can often lead to rapid and uncontrolled gelation.<sup>39,40</sup> This was shown through consistency measurements, where 4% Alg +  $\text{Ca}^{2+}$  had greater fluctuations in

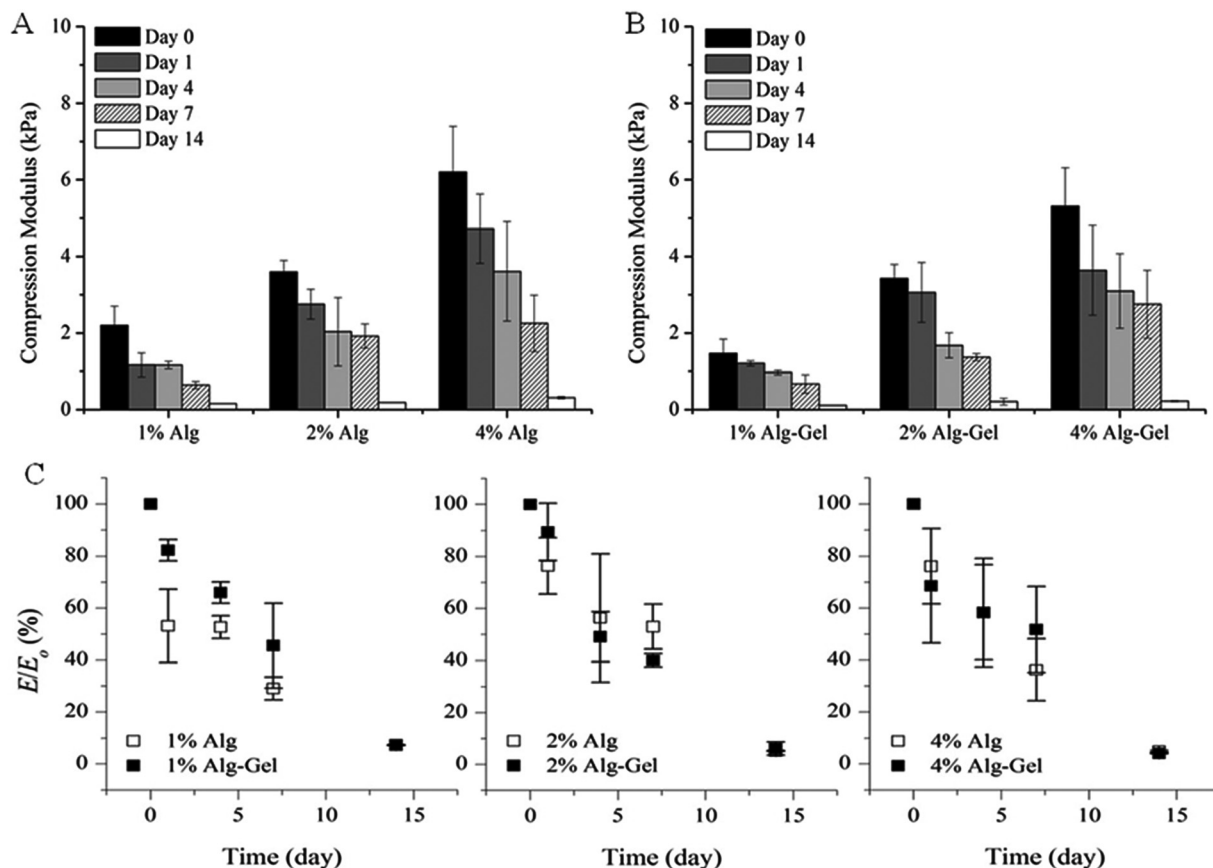


**Fig. 7** Compression modulus of (A) Alg; and (B) Alg-Gel in cell culture medium over 14 days. (C) Modulus remaining. Expressed as a percentage of the modulus ( $E/E_0$ ) at the specified time point relative to the initial modulus at day 0. Data represents mean  $\pm$  s.d.

extrusion force compared with water and Alg-Gel (which were similar to each other) indicating greater heterogeneity within the solution. As a result of the preparation process, the Alg +  $\text{Ca}^{2+}$  inks are inherently non-homogeneous. In the preparation of Alg +  $\text{Ca}^{2+}$  inks,  $\text{Ca}^{2+}$  cations are added to the Alg solution followed by a thorough mixing which results in formation of crosslinked gel fragments within the Alg ink solution. The fluctuations observed in Fig. 4 may be the result of these hydrogel fragments in the ink which gives the ink an inhomogeneous nature. Based on these results, although pre-crosslinking alginate inks exhibit gel-like characteristics, the consistency, viscosity and potential cytotoxicity precludes their use to print cells for fabricating implantable regenerative cell/scaffold constructs.

Alg-Gel was examined as an alternative formulation to pre-crosslinked alginate. By utilising the gelling characteristics of gelatin at low temperatures, the viscosity and storage modulus of alginate-based inks can be increased without addition of  $\text{Ca}^{2+}$ , thereby making these gels more bio-friendly to cells. Frequency sweep measurements indicated that Alg-Gel ink solutions exhibit gel-like characteristics at low temperatures and can be consistently extruded from a nozzle. This suggested that gelation took place homogeneously and more uniformly, allowing more controllable ink deposition. In addition, printed scaffolds of varied alginate concentrations illustrated

in Fig. 3 showed that scaffolds with well-defined pore diameter and filament width can be achieved using much lower alginate concentrations than with pre-crosslinked alginate. The frequency-independent storage modulus of the Alg-Gel ink ( $\sim 200$  Pa) is sufficient enough to sustain the weight of printed scaffold during the course of printing. It was observed that the gelation temperature for Alg-Gel solutions was lower than gelatin solutions alone (Fig. 2A). This was likely due to the lower concentration of gelatin when blended with alginate, leading to lesser formation of triple helices upon cooling.<sup>41</sup>

The mechanical property of a given scaffold is an important factor that influences the integrity of the scaffold post-printing,<sup>2,42</sup> ease of handling,<sup>43</sup> and also the biological behaviour of cells within the scaffold.<sup>37</sup> The scaffold's mechanical strength needs to be sufficient to support and maintain pore diameter for nutrient transfer to the cells. In some instances, it is favourable for the scaffold to degrade over time to facilitate biological functions as tissue is replaced.<sup>44</sup> The mechanical stiffness of Alg and Alg-Gel formations were tested by compression and indentation tests to study the mechanical performance of printed scaffolds. The former measures the modulus throughout the bulk of the sample, while the latter measures the local modulus closer to the surface of the sample. Consistent with the literature, both tests showed an



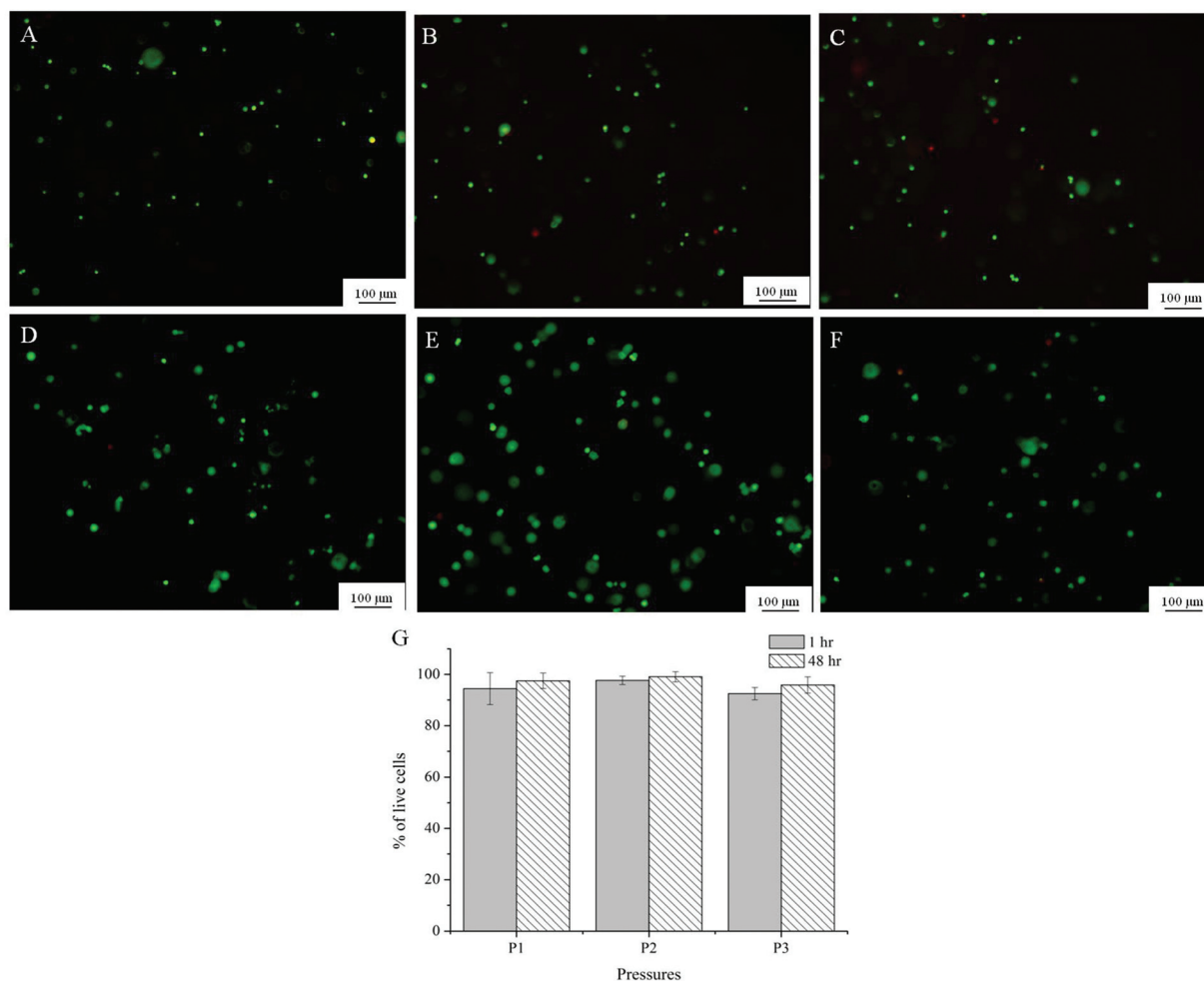


**Fig. 8** Representative images from Live/dead assay of Alg-Gel extruded at P1 (8 psi, A and D); P2 (16 psi, B and E); P3 (24 psi, C and F) after 1 hour (A–C) and 48 hours (D–F); (G) quantification of viability at 3 different pressures at 1 and 48 hour after printing.

increase in modulus with increasing alginate concentration due to the increase in the number of crosslinks and higher chain density.<sup>39,45</sup> The obtained compression modulus for alginate here was consistent with those reported in the literature (~4 kPa for 2% alginate).<sup>36</sup>

Noticeably, the compression modulus measured was lower than the indentation modulus across all samples. It has been reported that different experimental techniques for Young's modulus measurements may give inherently different values for the modulus of a sample. This difference between measured moduli is more profound when the sample is not homogeneous,<sup>46</sup> or has structural micro-defects. A study conducted by McKee *et al.*<sup>46</sup> compared the modulus of various soft tissues obtained through tensile and indentation testing and found that Young's modulus obtained in tensile tests were significantly higher than Young's modulus obtained in indentation. This was explained by the non-uniformity of natural soft tissues. The tensile test measures the combined response from all components of that tissue (*e.g.* cells, fibres and elastin), while indentation perturbs the tissue on the same

scale as the individual constituents. Both of these methods however, are relevant and necessary to fully understand the properties of the tissue.<sup>46</sup>

In this study, compression testing was used rather than the tensile test, but this technique still measures the macroscopic deformation of the entire sample. For the alginate sample crosslinked in CaCl<sub>2</sub> for 10 min, it is expected that regions closer to the sample–solution interface will crosslink first while the inner portion of the sample will take longer for Ca<sup>2+</sup> to diffuse. This may explain the higher indentation modulus measured across all sample given that unlike the compression, indentation measurements are performed on a localised region (~1 mm) and the indentation depth is only 0.2 mm. On the other hand, the compression test measures the mechanical behaviour of the entire sample that is more sensitive to defects and the overall degree of crosslinking.

An *in vitro* degradation study was conducted to examine the relationship between modulus and incubation time in cell culture media. Alginate is known to quickly lose its mechanical properties and reverse back to its soluble form through

ion exchange with monovalent cations,<sup>11</sup> while gelatin reverses to its soluble form at physiological temperature. Studies conducted by Shoichet *et al.*<sup>47</sup> observed a 40% decrease of modulus over 9 days using a 1.5% w/v alginate crosslinked for 4 h in a 1% w/v CaCl<sub>2</sub> solution. Crosslinked for 10 min, results from Fig. 6A and 7A showed that Alg loses more than 60% of its initial modulus after 7 days and continues to decrease throughout the period tested. The weight of Alg also decreased with time (mass loss ~14% and 22% for 1% and 4% Alg respectively). A similar trend was also observed in Alg-Gel samples but the rate of modulus loss was not noticeably faster than samples without gelatin. The percentage of mass loss however, was faster than Alg samples with 1% and 4% Alg-Gel showing a loss of around 57% and 36% respectively. This could be due to the presence of gelatin that dissolves at 37 °C. The stiffness and degradability of a scaffold are important factors for cell proliferation with some reports showing generally better proliferation in softer matrices than stiffer gels. This is mainly because in a less dense network structure, cells more easily overcome their surrounding structure and are able to move, grow, divide and differentiate.<sup>38,45,48,49</sup> Further studies will look at the effect of modulus and dissolution rate on cell proliferation and the possibility to deposit multiple cell types.

Live/dead cell assay showed that primary myoblasts maintained viability within the Alg-Gel scaffold even after being printed at pressures 2 to 3 times higher than pressures that would normally provide good resolution and filament size, as shown in Fig. 3. Previously, it has been reported that higher pressures increase the shear stress at the nozzle which damages the cell membrane and thus lowers cell viability after extrusion.<sup>6</sup> In contrast, cell viability across all the pressures used in this study was above 90% an hour following printing and was not significantly different even after 48 hours. This is in agreement with findings in the literature where cells still demonstrated good viability across varying pressures of extrusion.<sup>50,51</sup> This suggested that the pressure selected to print optimally for this formulation did not induce adverse cellular response and were appropriate for the selected cell type. The fact that the cells were surrounded within the gel may also shield them from the shear forces at the nozzle tip.<sup>51</sup> Cell proliferation was not observed from the Alg-Gel scaffolds within the time period tested. This may suggest that the cells require longer times to overcome their surrounding structure and proliferate. A study conducted by Gaetani *et al.*<sup>14</sup> reported an increase in the number of human cardiomyocyte progenitor cells (hCMPCs) within alginate matrices after 1 week of culture, whereas there were no signs of cell proliferation just after 24 hours in culture. Therefore, further studies into the proliferation and functions of these muscle cells will need to be conducted at longer periods of time.

The effect of low temperatures on encapsulated cells within the “ink” did not affect the cell viability. Since the cells were exposed to low temperatures (5 °C) for only a short period of time (10–15 min), the high percentage of viable cells suggested that they were able to restore cell functions when returned to

warm temperatures.<sup>52,53</sup> Collectively, this work has identified that hybrid Alg-Gel matrices provide an excellent substrate controllable for primary muscle cell growth while maintaining processability through physical properties inherent to the Alg component of the gel.

## 5. Conclusions

Ink formulation can be considered as one of the most important aspects of the bioprinting process. A suitable ‘bio-ink’ has to fulfill various rheological, mechanical and biological requirements during and after printing. The printability, mechanical properties and cell viability characteristics of alginate-based hydrogel scaffolds were explored using various analytical techniques. It was found that the pre-crosslinked alginate formulation consisting of alginate and CaCl<sub>2</sub> was not stable during the course of extrusion printing and the produced scaffolds were liquid-like with inconsistent pore diameter. On the other hand, by adding gelatin, the printability was enhanced considerably as shown by well defined structures and pore diameter. The consistency of each formulation during the extrusion printing process was measured by monitoring the force fluctuations. It was shown that Alg-Gel had lesser variations than Alg + Ca<sup>2+</sup> ink solutions. The rheological tests also confirmed the gel-like characteristics at low temperatures and over a wide range of frequency. Mechanical properties and degradation of hydrogel scaffolds was studied by performing compression and indentation tests on the hydrogel samples. The measured moduli obtained from compression and indentation was similar, ranging between 1.5 and 12 kPa as alginate concentration increased (day 0). The *in vitro* degradation tests were performed on Alg and Alg-Gel by monitoring the decay in modulus of hydrogels over time in cell culture media. A 50% drop in modulus was observed after 4 days and was decreased to more than 80% after 14 days. This was an important aspect that affected not only the stability of these printed gels in cell culture but also cell proliferation at later stages. An evaluation of cell viability from the undertaken preparation and printing processes showed that myoblast viability was unaffected by the extrusion pressure levels needed for extrusion printing of this myoblasts/Alg-Gel construct. The various characterisation techniques used here provide the criteria by which the printability of a hydrogel-based ink can be evaluated. As such, these techniques translate directly to the selection of other potential gel based systems for printing cell-laden hydrogels.

## Acknowledgements

This research was supported by the Australian Research Council, Super Science Fellowship Scheme, ARC Centre for Electromaterials Science (ACES) and NHMRC (Project 573430). The authors would like to acknowledge the Australian National Fabrication Facility (ANFF) for funding of the equipments, EMC facility at University of Wollongong (Innovation campus)

for microscopy analysis, Dr Stephen Beirne for the making of hydrogel moulds, ARC Fellowships to Gordon G. Wallace (Australian Laureate Fellow), and Simon E. Moulton (ARC QEII Fellow) are gratefully acknowledged.

## Notes and references

- 1 T. Billiet, M. Vandenhoute and J. Schelfhout, *et al.*, *Biomaterials*, 2012, **33**(26), 6020–6041.
- 2 N. E. Fedorovich, J. Alblas and J. R. De Wijn, *et al.*, *Tissue Eng.*, 2007, **13**(8), 1905–1925.
- 3 R. Landers and R. Mulhaupt, *Macromol. Mater. Eng.*, 2000, **82**, 17–21.
- 4 R. Landers, A. Pfister and U. Hübner, *et al.*, *J. Mater. Sci.*, 2002, **37**(15), 3107–3116.
- 5 S. Wüst, R. Müller and S. Hofmann, *J. Funct. Biomater.*, 2011, **2**(3), 119–154.
- 6 H. J. Kong, M. K. Smith and D. J. Mooney, *Biomaterials*, 2003, **24**(22), 4023–4029.
- 7 J. P. Frampton, M. R. Hynd and M. L. Shuler, *et al.*, *Biomed. Mater.*, 2011, **6**, 015002.
- 8 E. Rosellini, C. Cristallini and N. Barbani, *et al.*, *J. Biomed. Mater. Res., Part A*, 2009, **91**(2), 447–453.
- 9 Z. Dong, Q. Wang and Y. Du, *J. Membr. Sci.*, 2006, **280**(1–2), 37–44.
- 10 A. D. Augst, H. J. Kong and D. J. Mooney, *Macromol. Biosci.*, 2006, **6**(8), 623–633.
- 11 K. Y. Lee and D. J. Mooney, *Prog. Polym. Sci.*, 2012, **37**(1), 106–126.
- 12 P. Matricardi, C. D. Meo and T. Coviello, *et al.*, *Expert Opin. Drug Delivery*, 2008, **5**(4), 417–425.
- 13 K. Y. Lee and D. J. Mooney, *Chem. Rev.*, 2001, **101**, 1869–1879.
- 14 R. Gaetani, P. A. Doevendans and C. H. G. Metz, *et al.*, *Biomaterials*, 2012, **33**, 1782–1790.
- 15 N. C. Hunt, A. M. Smith and U. Gbureck, *et al.*, *Acta Biomater.*, 2010, **6**(9), 3649–3656.
- 16 L. Dreesmann, M. Ahlers and B. Schlosshauer, *Biomaterials*, 2007, **28**(36), 5536–5543.
- 17 K. Sandrasegaran, C. Lall and A. Rajesh, *et al.*, *Am. J. Roentgenol.*, 2005, **184**(2), 475–480.
- 18 B. Balakrishnan, M. Mohanty and P. R. Umashankar, *et al.*, *Biomaterials*, 2005, **26**(32), 6335–6342.
- 19 M. Djabourov, J. Leblond and P. Papon, *J. Phys.*, 1988, **49**, 319–332.
- 20 W. Carvalho and M. Djabourov, *Rheol. Acta*, 1997, **36**(6), 591–609.
- 21 R. Landers, U. Hübner and R. Schmelzeisen, *et al.*, *Biomaterials*, 2002, **23**(23), 4437–4447.
- 22 N. W. Fadnavis, G. Sheelu and B. M. Kumar, *et al.*, *Biotechnol. Prog.*, 2003, **19**(2), 557–564.
- 23 L. Fan, Y. Du and R. Huang, *et al.*, *J. Appl. Polym. Sci.*, 2005, **96**(5), 1625–1629.
- 24 Y. S. Choi, S. R. Hong and Y. M. Lee, *et al.*, *Biomaterials*, 1999, **20**(5), 409–417.
- 25 S. Li, Y. Yan and Z. Xiong, *et al.*, *J. Bioact. Compat. Polym.*, 2009, **24**(1 suppl), 84–99.
- 26 Y. Yan, X. Wang and Z. Xiong, *et al.*, *J. Bioact. Compat. Polym.*, 2005, **20**(3), 259–269.
- 27 S. Li, Z. Xiong and X. Wang, *et al.*, *J. Bioact. Compat. Polym.*, 2009, **24**, 249–265.
- 28 D. L. Cohen, W. Lo and A. Tsavaris, *et al.*, *Tissue Eng., Part C*, 2011, **17**(2), 239–248.
- 29 J. W. Harding and I. N. Sneddon, *Math. Proc. Cambridge Philos. Soc.*, 1945, **41**(01), 16–26.
- 30 J. A. Rowley, G. Madlambayan and D. J. Mooney, *Biomaterials*, 1999, **20**(1), 45–53.
- 31 N. O. Dhoot, C. A. Tobias and I. Fischer, *et al.*, *J. Biomed. Mater. Res., Part A*, 2004, **71**(2), 191–200.
- 32 P. K. Kreeger, T. K. Woodruff and L. D. Shea, *Mol. Cell. Endocrinol.*, 2003, **205**(1–2), 1–10.
- 33 R. Kapsa, A. Quigley and G. S. Lynch, *et al.*, *Hum. Gene Ther.*, 2001, **12**(6), 629–642.
- 34 S. Jin-Hyung, L. Jung-Seob and K. Jong Young, *et al.*, *J. Micromech. Microeng.*, 2012, **22**(8), 085014.
- 35 J. Kundu, J.-H. Shim and J. Jang, *et al.*, *J. Tissue Eng. Regener. Med.*, 2013.
- 36 L. Q. Wan, J. Jiang and D. E. Arnold, *et al.*, *Cell. Mol. Bioeng.*, 2008, **1**(1), 93–102.
- 37 M. D. Bootman, A. M. Holmes and H. L. Roderick, *Calcium Signalling and Regulation of Cell Function*. eLS, John Wiley & Sons, Ltd, 2001.
- 38 N. Cao, X. B. Chen and D. J. Schreyer, *ISRN Chem. Eng.*, 2012, **2012**, 1–9.
- 39 C. K. Kuo and P. X. Ma, *Biomaterials*, 2001, **22**(6), 511–521.
- 40 C. K. Kuo and P. X. Ma, *J. Biomed. Mater. Res.*, 2007, **84A**, 899–907.
- 41 S. M. Tosh and A. G. Marangoni, *Appl. Phys. Lett.*, 2004, **84**(21), 4242–4244.
- 42 D. W. Hutmacher, *Biomaterials*, 2000, **21**(24), 2529–2543.
- 43 E. Sachlos and J. T. Czernuszka, *Eur. Cells Mater.*, 2003, **5**, 29–40.
- 44 S. Khalil and W. Sun, *J. Biomech. Eng.*, 2009, **131**(11), 111002–8.
- 45 A. Banerjee, M. Arha and S. Choudhary, *et al.*, *Biomaterials*, 2009, **30**(27), 4695–4699.
- 46 C. T. McKee, J. A. Last and P. Russell, *et al.*, *Tissue Eng., Part B*, 2011, **17**(3), 155–164.
- 47 M. S. Shoichet, R. H. Li and M. L. White, *et al.*, *Biotechnol. Bioeng.*, 1996, **50**, 374–381.
- 48 T. P. Kraehenbuehl, P. Zammaretti and A. J. Van der Vlies, *et al.*, *Biomaterials*, 2008, **29**(18), 2757–2766.
- 49 K. Bott, Z. Upton and K. Schrobback, *et al.*, *Biomaterials*, 2010, **31**(32), 8454–8464.
- 50 J. T. Connelly, A. J. García and M. E. Levenston, *Biomaterials*, 2007, **28**(6), 1071–1083.
- 51 J. Cheng, F. Lin and H. Liu, *et al.*, *J. Manufac. Sci. Eng.*, 2008, **130**(2), 021014–5.
- 52 B. J. Fuller, *CryoLetters*, 2003, **24**, 95–102.
- 53 B. C. Heng, K. J. Vinoth and H. Liu, *et al.*, *Int. J. Med. Sci.*, 2006, **3**, 124–129.